

1 **Supplementary Materials**

2

3 ***Fgf9* regulates bone marrow mesenchymal stem cell fate and bone-fat**
4 **balance in osteoporosis by PI3K/AKT/Hippo and MEK/ERK signaling**

5

6 Mingmei Chen¹, Hui Liang¹, Min Wu², Haoyang Ge¹, Yan Ma³, Yan Shen¹, Shunyuan
7 Lu¹, Chunling Shen¹, Hongxin Zhang¹, Zhugang Wang^{1*}, Lingyun Tang^{1*}

8

9

10

11 **Table of Contents**

12 **Figure S1. *Fgf9* in bone marrow clusters.**

13 **Figure S2. *Fgf9*^{S99N} mutation mitigates BMAT accumulation in adult mice.**

14 **Figure S3. *Fgf9*^{S99N} mutation involves in bone-fat balance.**

15 **Figure S4. *Fgf9* regulates BMSCs differentiation both in mice and rat.**

16 **Figure S5. Differentiation of *OE-Ctrl/OE-Fgf9* BMSCs in vivo.**

17 **Figure S6. Analysis of DEGs and mRNA level of bone-fat related genes.**

18 **Figure S7. Quantitative results of protein levels from Figure 6.**

19 **Figure S8. *Fgf9* regulates BMSCs through FGFR1, PI3K/AKT and Hippo**
20 **pathways.**

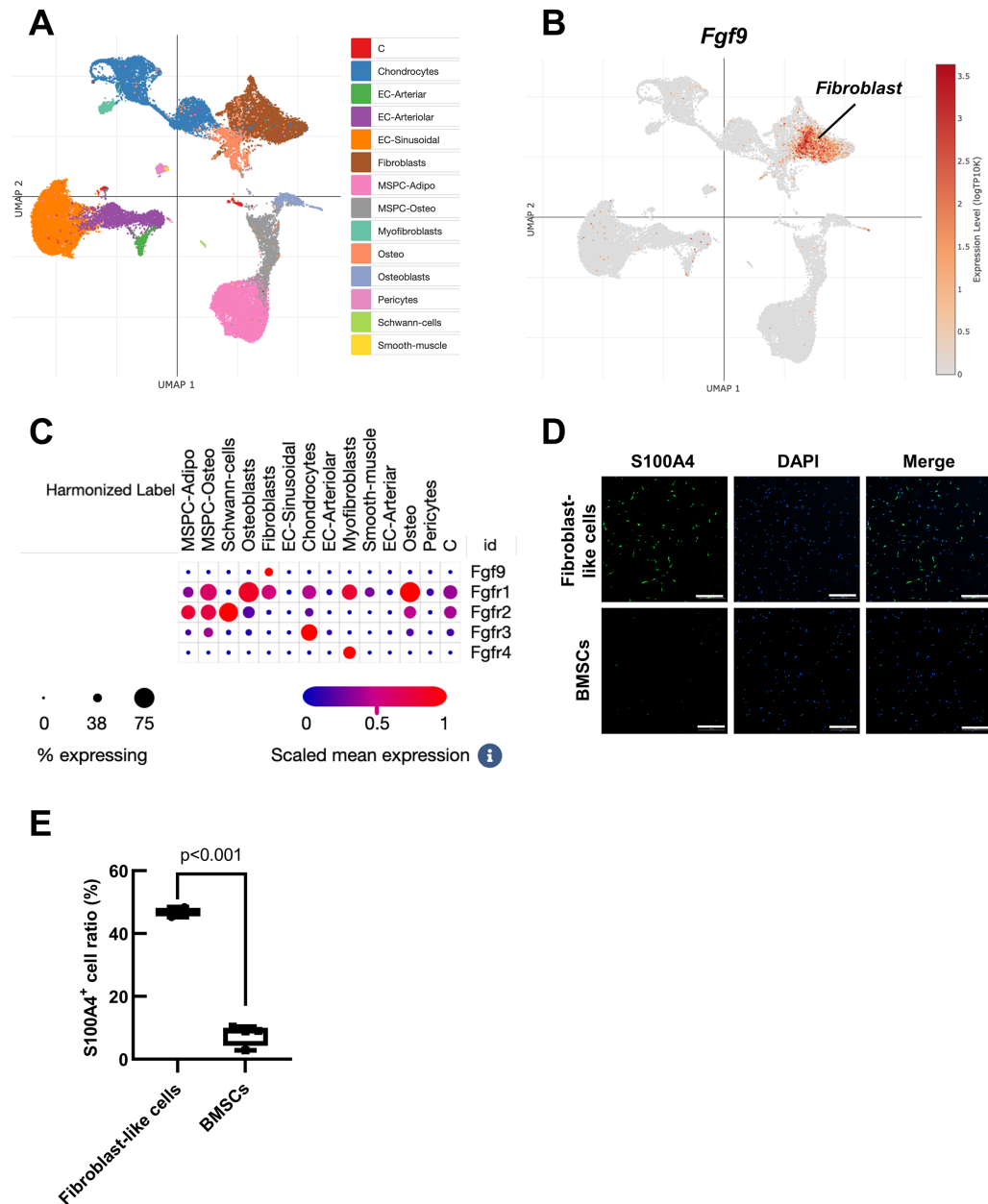
21 **Figure S9. Quantitative results of phosphorylated protein levels from Figure 8.**

22 **Table S1. Inhibitors used for signaling transduction.**

23 **Table S2. Primers used for mRNA expression detection and genotyping.**

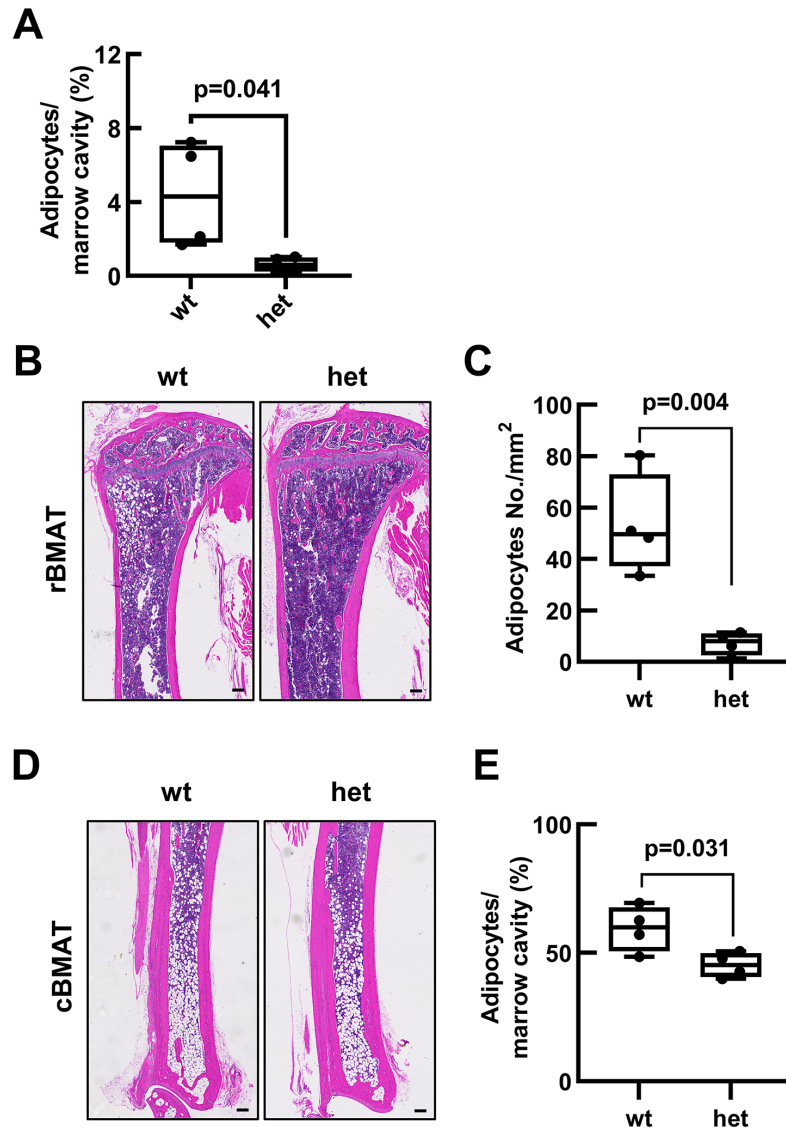
24 **Table S3. Antibodies information.**

25



1
2 **Figure S1. *Fgf9* in bone marrow clusters.** (A) UMAP visualization of all bone
3 marrow cells from the integrated analysis, color-coded based on the clusters. (B)
4 Distribution of *Fgf9* in bone marrow stroma cell clusters. (C) Expression of *Fgf9* and
5 *Fgfrs* in bone marrow clusters. The size of dots represents the percentage of expression;
6 red and blue represent the level of scaled mean expression. (D) Immunofluorescence
7 staining of S100A4 in Fibroblast-like cells and BMSCs. (E) S100A4⁺ cell ratio in
8 Fibroblast-like cells and BMSCs. Data are analyzed by Student's t-test and shown as
9 boxplots (median ± interquartile range). Scale bars represent 300 μm.

1



2

3 **Figure S2. *Fgf9*^{S99N} mutation mitigates BMAT accumulation in adult mice. (A)**

4 Statistical analysis of femur adipocytes area in 4-month-old wt and het mice. **(B)** H&E

5 staining of rBMAT in tibiae from 4-month-old male wild-type and heterozygous mice.

6 **(C)** Statistical analysis of rBMAT adipocyte number in 4-month-old wt and het mice.

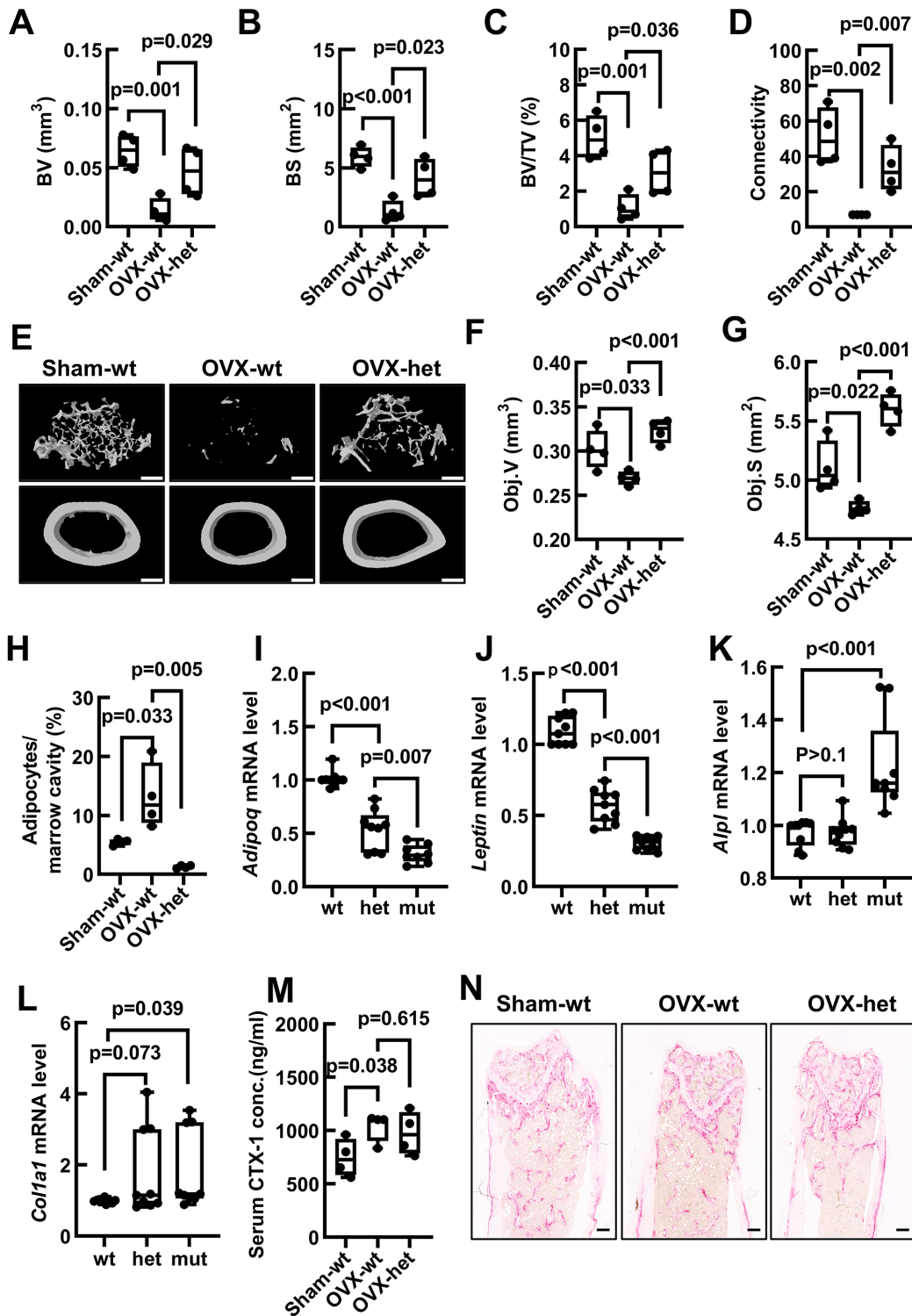
7 **(D)** H&E staining of cBMAT in tibiae from 4-month-old male wt and het mice. **(E)**

8 Statistical analysis of cBMAT adipocytes area in 4-month-old wt and het mice. Data

9 are analyzed by Student's t-test and shown as boxplots (median \pm interquartile range),

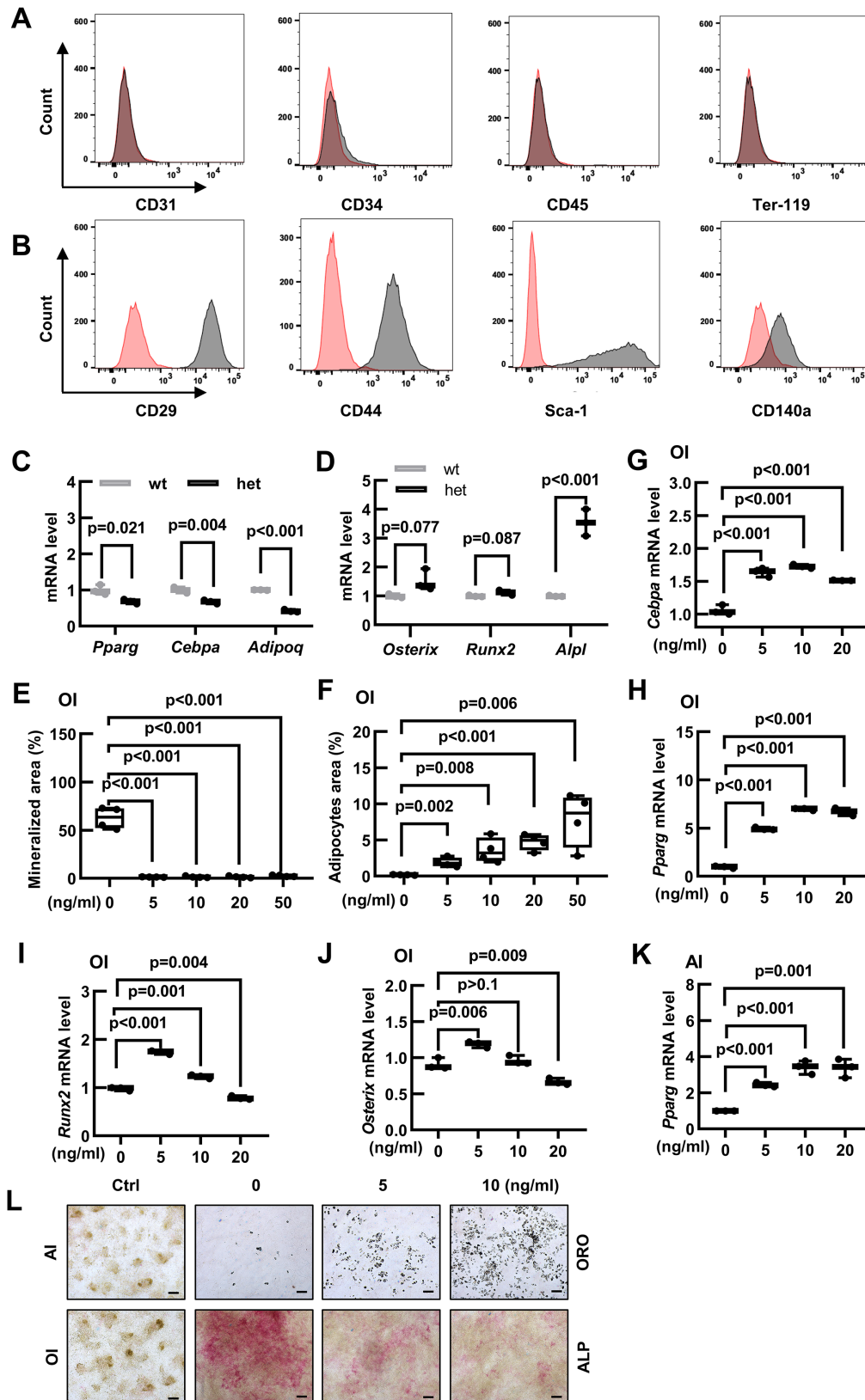
10 $n = 4$ mice in each group. Scale bars represent 200 μm .

11



3 **Figure S3. *Fgf9*^{S99N} mutation involves in bone-fat balance.** (A-D) Bone volume (BV),
 4 Bone surface (BS), Percent bone volume (BV/TV), and Connectivity (Conn) were
 5 determined by micro-CT analysis. (E) Micro-CT images of the lateral-view of
 6 trabecular bone of the metaphyseal region (above) and top-view cortical bone (below),

1 scale bars represent 1 mm. **(F, G)** Cortical bone parameters were measured including
2 Object volume (Obj.V) and Object surface (Obj.S). **(H)** Quantification analysis of
3 femur adipocytes area / bone marrow cavity area percentage in Sham-wt, OVX-wt, and
4 OVX-het mice. **(I-L)** Relative mRNA level of *Adipoq*, *Leptin*, *Alpl*, and *Coll1a1* in
5 femurs of neonatal wt, het, and homozygous (mut) mice. **(M)** Quantification analysis
6 of serum CTX-1 level in Sham-wt, OVX-wt, and OVX-het mice by ELISA. **(N)**
7 Representative images of TRAP staining in femurs of Sham-wt, OVX-wt, and OVX-
8 het mice, scale bars represent 200 μ m. Data are analyzed by Student's t-test and shown
9 as boxplots (median \pm interquartile range). In (A) - (H), (M), and (N), n = 4 in each
10 group. In (I) - (L), n = 3 mice with 3 biological replicates in each group.
11



1

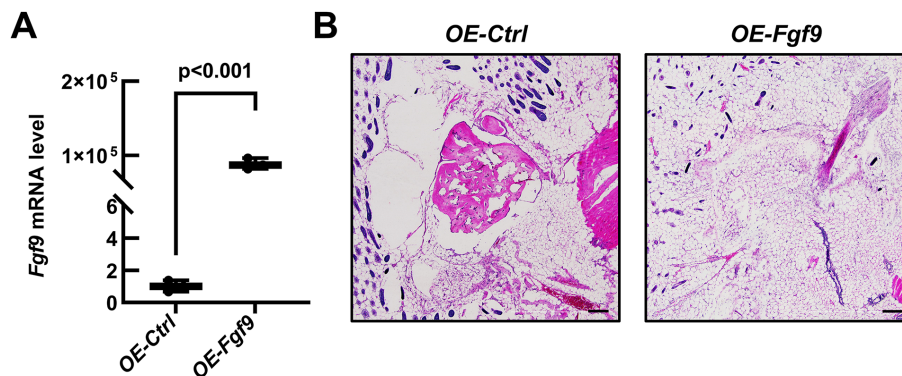
2 **Figure S4. *Fgf9* regulates BMSCs differentiation both in mice and rat. (A, B)**

3 Negative surface markers (CD31, CD34, CD45, and Ter-119) (A) and positive markers

4 (CD29, CD44, Sca-1, and CD140a) (B) of BMSCs were characterized using flow

1 cytometry. Isomorphous antibodies used as negative control. (C, D) Relative mRNA
 2 levels of *Cebpa*, *Pparg*, and *Adipoq* (C), *Osterix*, *Runx2*, and *Alpl* (D) in BMSCs from
 3 20-month-old wt and het mice. (E-F) Quantification measurement of mineralization
 4 area and adipocytes area under OI condition. n = 4 independent experiments with
 5 biological replicates. (G-J) Relative mRNA levels of *Runx2*, *Osterix*, *Cebpa*, and *Pparg*
 6 in osteogenesis induction, while BMSCs were cultured with different concentrations of
 7 FGF9 (0, 5, 10 and 20 ng/ml). n = 3 biological replicates over three independent
 8 experiments. (K) Under adipogenesis induction, relative mRNA level of *Pparg* in
 9 BMSCs with different FGF9 concentrations (0, 5, 10 and 20 ng/ml). n = 3 biological
 10 replicates over three independent experiments. (L) ALP staining and Oil Red O staining
 11 of rat BMSCs in OI and AI medium with different concentrations of FGF9 (0, 5 and 10
 12 ng/ml). Data are analyzed by Student's t-test and shown as boxplots (median ±
 13 interquartile range). Scale bars represent 200 μm.

14
 15

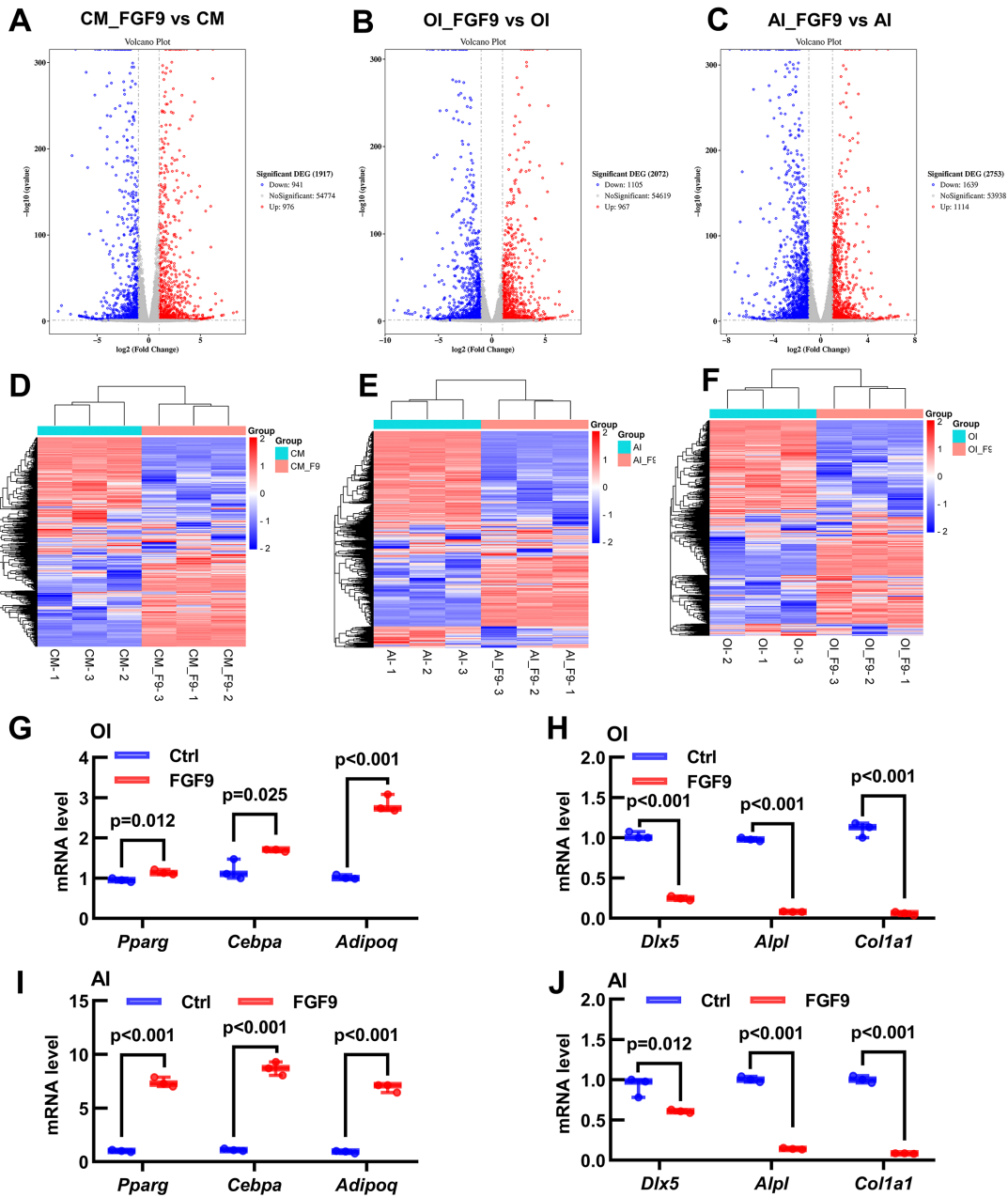


16

17 **Figure S5. Differentiation of *OE-Ctrl/OE-Fgf9* BMSCs in vivo.** (A) mRNA
 18 expression level of *Fgf9* increased dramatically after transfection. n = 3 biological
 19 replicates over three independent experiments. (B) After subcutaneous injection for 5
 20 weeks, smaller magnifications of H&E staining, n = 3 mice. Data are analyzed by
 21 Student's t-test and shown as boxplots (median ± interquartile range). Scale bars
 22 represent 200 μm.

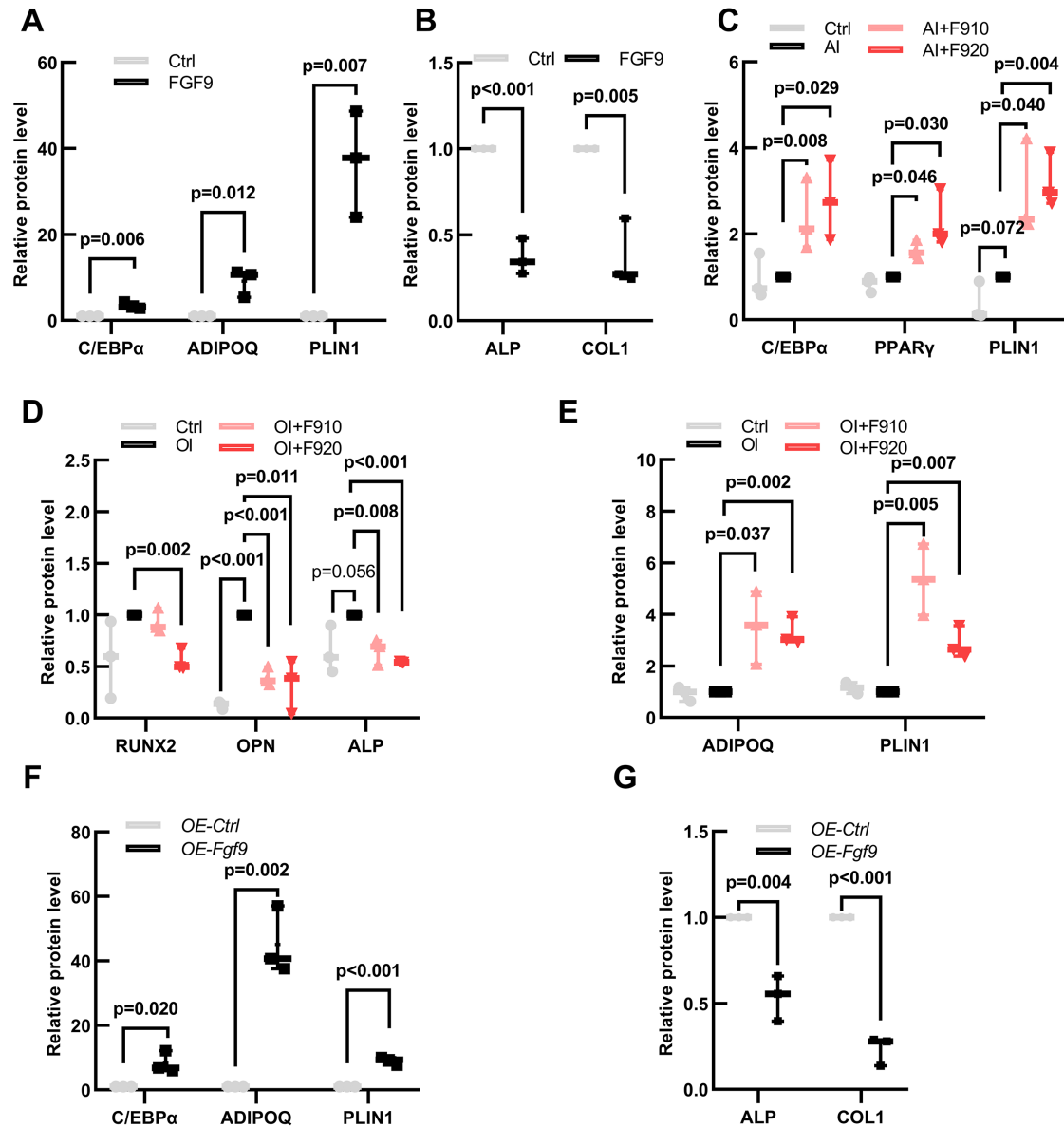
23

24



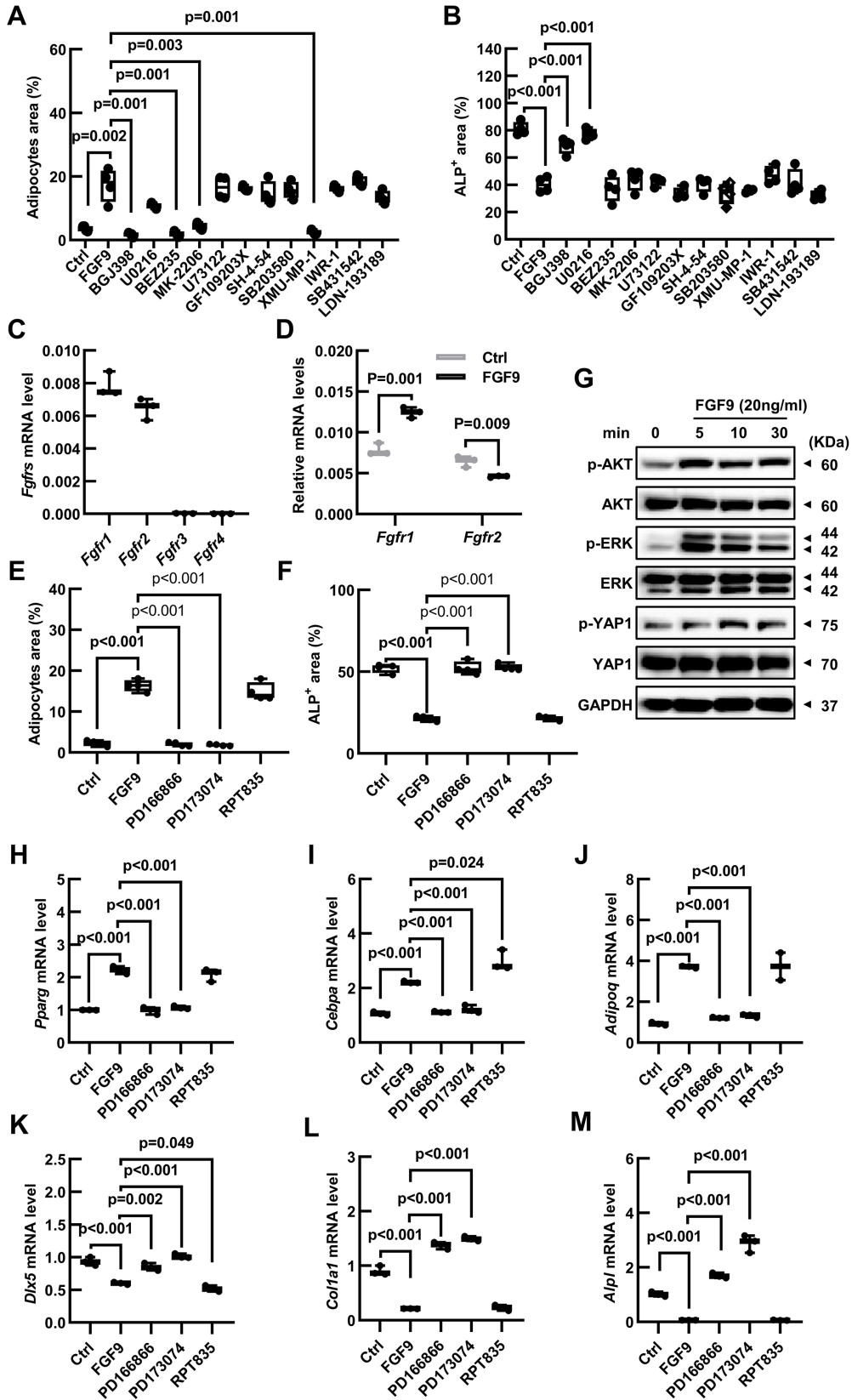
1
2 **Figure S6. Analysis of DEGs and mRNA level of bone-fat related genes. (A-C)**
3 Volcano plots exhibited significantly DEGs under CM (976 up-regulated and 941
4 down-regulated genes) (A), OI (967 up-regulated and 1105 down-regulated genes) (B)
5 and AI (1114 up-regulated and 1639 down-regulated genes) (C) conditions. (D-F)
6 Heatmaps of DEGs showed changes between control and experimental groups under
7 CM (D), AI (E) and OI (F) conditions. (G-H) Relative mRNA level of *Pparg*, *Cebpa*,
8 *Adipoq* (G), and *Dlx5*, *Alpl*, and *Colla1* (H) in BMSCs cultured with FGF9 under OI
9 conditions. (I-J) Relative mRNA level of *Pparg*, *Cebpa*, *Adipoq* (I), and *Dlx5*, *Alpl*,
10 and *Colla1* (J) in BMSCs cultured with FGF9 under AI conditions. n = 3 biological

1 replicates over three independent experiments. DEGs are defined as $|\text{Log}_2\text{FC}| \geq 1$ and
 2 adjusted P-value ≤ 0.05 . Data are analyzed by Student's t-test and shown as boxplots
 3 (median \pm interquartile range).
 4



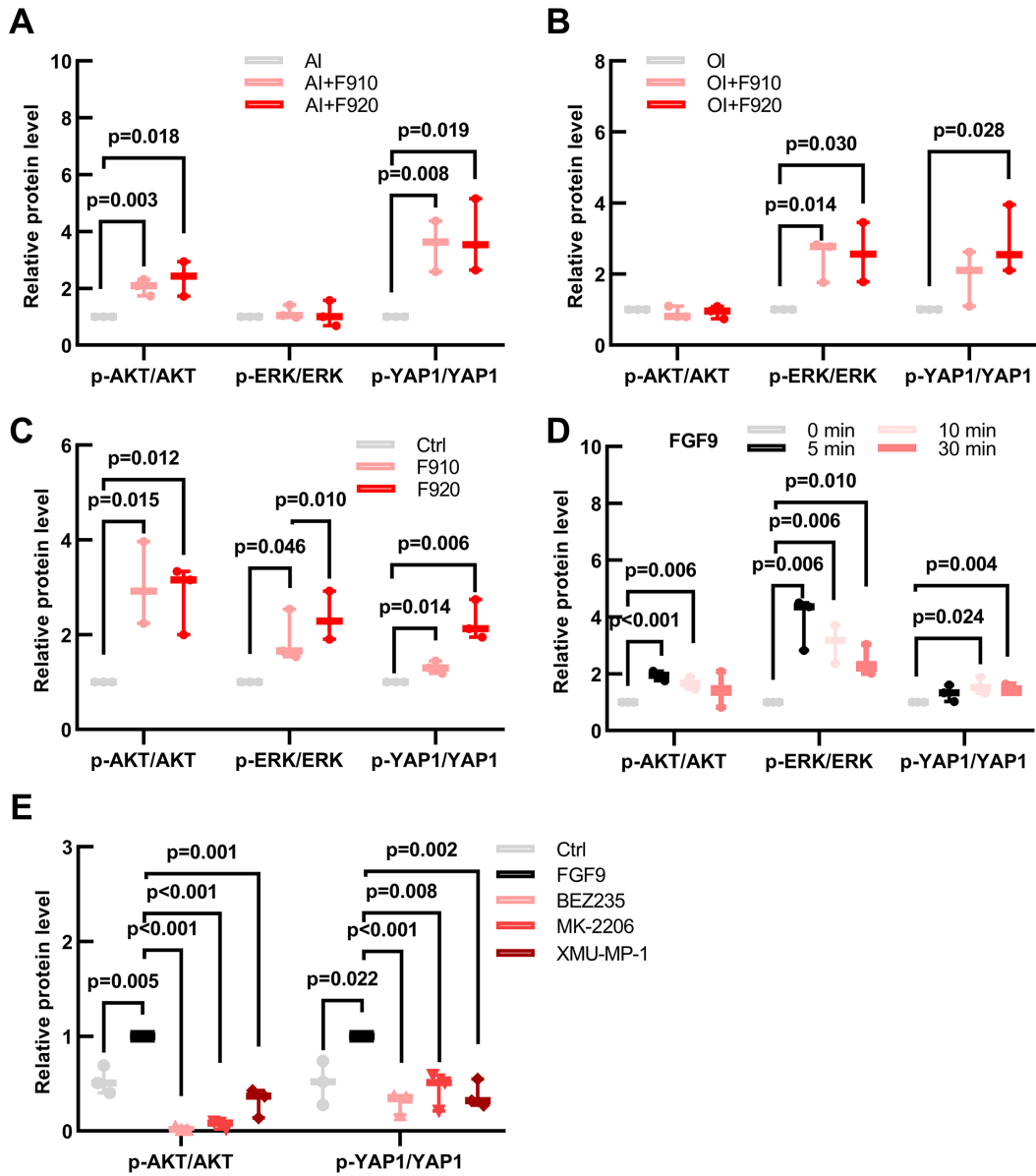
5 **Figure S7. Quantitative results of protein levels from Figure 6. (A-B)** Protein levels
 6 of adipogenic genes (C/EBPα, ADIPOQ, PLIN1) and osteogenic genes (ALP, COL1)
 7 were quantitatively analyzed in BMSCs under CM conditions with/without FGF9
 8 stimulation referring to Figure 6G. **(C)** Protein levels of adipogenic genes (C/EBPα,
 9 PPARγ, PLIN1) were quantitatively analyzed in BMSCs under AI conditions
 10 with/without FGF9 stimulation referring to Figure 6H. **(D-E)** Protein levels of

1 osteogenic genes (RUNX2, OPN, ALP) and adipogenic genes (ADIPOQ, PLIN1) were
2 quantitatively analyzed in BMSCs under OI conditions with/without FGF9 stimulation
3 referring to Figure 6I. **(F-G)** Protein levels of C/EBP α , ADIPOQ, PLIN1, ALP, and
4 COL1 in *OE-Ctrl* and *OE-Fgf9* BMSCs were quantitatively measured referring to
5 Figure 6L. n = 3 biological replicates over three independent experiments. Data are
6 analyzed by Student's t-test and shown as boxplots (median \pm interquartile range).
7
8



2 **Figure S8. *Fgf9* regulates BMSCs through FGFR1, PI3K/AKT and Hippo**
 3 **pathways. (A-B) Quantification measurement of adipocytes area under AI conditions**

1 (A) and ALP-positive area under OI conditions (B) in BMSCs stimulated with 20 ng/ml
2 FGF9 and inhibitors. n = 4 independent experiments with biological replicates. (C)
3 mRNA level of *Fgfr1-4* in BMSCs under CM conditions. (D) mRNA expression level
4 of *Fgfr1* and *Fgfr2* in BMSCs with/without FGF9 stimulation. (E-F) Quantification
5 measurement of adipocytes area under AI conditions (E) and ALP-positive area under
6 OI conditions (F) in BMSCs stimulated with 20 ng/ml FGF9 and inhibitors (FGFR1,
7 FGFR2). n = 4 independent experiments with biological replicates. (G) Immunoblotting
8 analysis showed the phosphorylated and total protein levels of ERK, AKT, and YAP1
9 in BMSCs stimulated with 20 ng/ml FGF9 for different time periods (0, 5, 10, and 30
10 min). (H-M) Relative mRNA levels of *Cebpa*, *Pparg*, *Adipoq*, *Dlx5*, *Alpl*, and *Colla1*
11 in BMSCs stimulated with 20 ng/ml FGF9 and inhibitors (FGFR1, FGFR2) under CM
12 conditions for 4 days, n = 3 biological replicates over three independent experiments.
13 Data are analyzed by Student's t-test and shown as boxplots (median \pm interquartile
14 range).
15



2 **Figure S9. Quantitative results of phosphorylated protein levels from Figure 8. (A-**
 3 **B)** Quantification measurement of the phosphorylated protein levels/total protein levels
 4 of ERK, AKT, and YAP1 in BMSCs with FGF9 stimulation (0, 10, and 20 ng/ml) under
 5 AI (A) or OI (B) conditions for 6 days, referring to Figure 8E. (C) Quantification
 6 measurement of the phosphorylated/total protein levels of ERK, AKT, and YAP1 in
 7 BMSCs stimulated with FGF9 (0, 10, and 20 ng/ml). BMSCs were cultured for 4 days
 8 under CM conditions, referring to Figure 8F. (D) Quantitative analysis of the
 9 phosphorylated protein levels/total protein levels of ERK, AKT, and YAP1 in BMSCs
 10 stimulated with 20 ng/ml FGF9 for different time periods (0, 5, 10, and 30 min),

1 referring to Figure S8G. **(E)** BMSCs were pre-treated with inhibitors for 10 hours and
2 stimulated with 20 ng/ml FGF9 for 10min, and the phosphorylated/total protein levels
3 of AKT and YAP1 in BMSCs were quantified, referring to Figure 8G. n = 3 biological
4 replicates over three independent experiments. Data are analyzed by Student's t-test and
5 shown as boxplots (median \pm interquartile range).
6

1

2 **Table S1. Inhibitors used for signaling transduction.**

	Inhibitor	Targets	Working Con (μM)
1	BGJ398	FGFRs	1.5
2	U0126	MEK	10
3	SB203580	P38	10
4	BEZ235	PI3K, mTOR	1
5	MK-2206	Akt1/2/3	2
6	U73122	PLC-γ	8
7	GF10920X	PKC	1
8	IWR-1-endo	Wnt	10
9	XMU-MP-1	Hippo	5
10	LDN-193189	BMP	0.2
11	SB431542	TGF-β	10
12	SH-4-54	STAT3&5	1
13	PD166866	FGFR1	0.25
14	PD173074	FGFR1	0.1
15	RPT835	FGFR2	10

3

4

1 **Table S2. Primers used for mRNA expression detection and genotyping.**

Gene	Forward primer	Reverse primer
<i>Osterix</i>	TGATGGGCTGCAAGGGACACTG	TTGGGCTTATAGACATCTTGGGGTAGGA
<i>Runx2</i>	GCGGACGAGGCAAGAGTTTC	AGCGGCGTGGTGGAGTGGAT
<i>Dlx5</i>	CGGCTACTGCTCTCCTACC	ATTCACCATCCTCACCTCTGG
<i>Alpl</i>	ACCAATGTAGCCAAGAATGTCA	CGTTATCCGAGTACCAGTCCC
<i>Colla1</i>	GCATGAGCCGAAGCTAACCC	GTGGCAGATACAGATCAAGCATAACC
<i>Cebpa</i>	GTTAGCCATGTGGTAGGAGACA	CCCAGCCGTTAGTGAAGAGT
<i>Pparg</i>	GAGCACTTCACAAGAAATTACC	AATGCTGGAGAAATCAACTG
<i>Adipoq</i>	CTCCACCCAAGGGAACCTTGT	TAGGACCAAGAAGACCTGCATC
<i>Leptin</i>	GTGGCTTTGGTCCTATCTGTC	CGTGTGTGAAATGTCATTGATCC
<i>Fgf9</i>	GCAGTCACGGACTTGGATCAT	TTCTCGTTCATGCCGAGGTAG
<i>Fgfr1</i>	GGATTCTGTGGTGCCTTCTGAC	CAAGTTGTCTGGCCCGAT
<i>Fgfr2</i>	ACCACACCTACCACCTCGAT	GGCATCGCTGTAAACCTTGC
<i>Fgfr3</i>	CTCAGAGGCTGCAAGTGCTAA	CGGGCGAGTCCAATAAGG
<i>Fgfr4</i>	CCGTGGCTGTGAAGATGCTGAA	GCAGGTTGATGATGTTCTTGTGTCTT
<i>β-actin</i>	CTGGCCGGGACCTGACAGACTACC	ATCGGAACCGCTCGTTGCCAATAG
Genotyping	CACTGGGCTCTAACTCTTCTGTCTGC	CTACATCACCATAAGGACCTACCAAGC
		TCCGATTGTCTGAGTAGGTGTCATTC

2

3

1 **Table S3. Antibodies information.**

	Name	Cat.NO.	Dilution
1	Anti-p-p44/42 MAPK (Erk1/2) (Thr202/Tyr204) (D13.14.4E)	CST, 4370	WB 1:1000
2	Anti-p44/42 MAPK (Erk1/2) (137F5)	CST, 4695	WB 1:1000
3	Anti-p-Akt (Ser473) (D9E)	CST, 4060	WB 1:1000
4	Anti-AKT	CST, 9272	WB 1:1000
5	Anti-p-YAP1 (Ser397)	Proteintech, 29018-1-AP	WB 1:1000
6	Anti-YAP1	Proteintech, 13584-1-AP	WB 1:1000
7	Anti-C/EBPα	Abcam, ab40764	WB 1:1000
8	Anti-ADIPOQ	Abcam, ab22554	WB 1:1000
9	Anti-PLIN1	Sigma, P1998	WB 1:1000, IF 1:100
10	Anti-PPARγ	CST, 2443	WB 1:1000
11	Anti-RUNX2	Abcam, ab76956	WB 1:1000
12	Anti-ALP	Proteintech, 11187-1-AP	WB 1:1000
13	Anti-OPN	R&D, AF808	WB 1:1000, IF 1:100
14	Anti-COL1	Abcam, ab308221	WB 1:1000
15	Anti-FGF9 (FG9-77)	Invitrogen, MA1-24684	WB 1:1000
16	Anti-S100A4	Proteintech, 16105-1-AP	IF 1:100
17	Anti-GAPDH	Sangon, D110016	WB 1:1000
18	Anti-Goat IgG H&L	Abcam, ab150129	IF 1:500
19	Anti-Rabbit IgG H&L	Invitrogen, A32740	IF 1:500

